Wastewater disposal and earthquake swarm activity at the southern end of the Central Valley, California,

T.H.W. Goebel, S.M. Hosseini, F. Cappa, E. Hauksson, J.-P. Ampuero, F. Aminzadeh, J.B. Saleeby

AGU PUBLICATIONS

Geophysical Research Letters

RESEARCH LETTER
10.1002/2015GL066948

Key Points:
- Anomalous swarm activity associated with White Wolf fault
- Induced seismicity likely caused by localized pressure increase along a seismically active fault
- Induced seismicity may be masked by natural earthquake activity in California

Supporting Information:
- Supporting Information S1
- Tables S1–S8
- Movie S1
- Movie S2
- Figures S1–S22

Correspondence to:
T. H. W. Goebel,
tgoebel@ucsc.edu

Citation:
Goebel, T. H. W., S. M. Hosseini, F. Cappa, E. Hauksson, J. P. Ampuero, F. Aminzadeh, and J. B. Saleeby (2016), Wastewater disposal and earthquake swarm activity at the southern end of the Central Valley, California, *Geophys. Res. Lett.*, *43*, 1092–1099, doi:10.1002/2015GL066948.

Received 8 NOV 2015
Accepted 16 JAN 2016
Accepted article online 22 JAN 2016
Published online 4 FEB 2016

Wastewater disposal and earthquake swarm activity at the southern end of the Central Valley, California

T. H. W. Goebel[1,2], S. M. Hosseini[3], F. Cappa[4,5], E. Hauksson[1], J. P. Ampuero[1], F. Aminzadeh[3], and J. B. Saleeby[1]

[1]Division of Geological and Planetary Sciences, California Institute of Technology, Pasadena, California, USA, [2]Now at Department of Earth and Planetary Sciences, University of California, Santa Cruz, California, USA, [3]Department of Chemical Engineering and Material Sciences, University of Southern California, Los Angeles, California, USA, [4]Geoazur Laboratory, University of Nice Sophia Antipolis, Nice, France, [5]Institut Universitaire de France, Paris, France

Abstract Fracture and fault zones can channel fluid flow and transmit injection-induced pore pressure changes over large distances (>km), at which seismicity is rarely suspected to be human induced. We use seismicity analysis and hydrogeological models to examine the role of seismically active faults in inducing earthquakes. We analyze a potentially injection-induced earthquake swarm with three events above *M*4 near the White Wolf fault (WWF). The swarm deviates from classic main aftershock behavior, exhibiting uncharacteristically low Gutenberg-Richter *b* of 0.6, and systematic migration patterns. Some smaller events occurred southeast of the WWF in an area of several disposal wells, one of which became active just 5 months before the main swarm activity. Hydrogeological modeling revealed that wastewater disposal likely contributed to seismicity via localized pressure increase along a seismically active fault. Our results suggest that induced seismicity may remain undetected in California without detailed analysis of local geologic setting, seismicity, and fluid diffusion.

1. Introduction

Fluid injection into hydrocarbon and geothermal reservoirs can change the local stress field potentially causing earthquakes at several kilometers distance, both immediately and months to years after peak injection [e.g., *Hsieh and Bredehoeft*, 1981; *Bourouis and Bernard*, 2007; *Keranen et al.*, 2013; *Kim*, 2013; *Martínez-Garzón et al.*, 2014; *Schoenball et al.*, 2014; *Rubinstein et al.*, 2014]. Injection-induced fault slip is, in addition to poroelastic stress changes, commonly attributed to an increase in pore pressure, which reduces the frictional resistance on fault surfaces [e.g., *Healy et al.*, 1968; *Hsieh and Bredehoeft*, 1981; *Ellsworth*, 2013; *Keranen et al.*, 2013]. In recent years, induced earthquakes have been observed in the proximity of many high-volume wastewater disposal (WD) wells in the central U.S. [e.g., *Horton*, 2012; *Frohlich and Brunt*, 2013; *Keranen et al.*, 2013; *Kim*, 2013; *Skoumal et al.*, 2014]. Many of the identified injection wells responsible for inducing seismicity are suspected to inject at depth close to the upper basement surface, where critically stressed faults slip more easily when exposed to changing pressures and earthquake ruptures can grow to larger sizes than in sedimentary basins [e.g., *Das and Scholz*, 1983; *Horton*, 2012; *Keranen et al.*, 2013; *Kim*, 2013; *Ellsworth*, 2013].

While many previous studies focused on regions within the central and eastern U.S., where induced event detection is facilitated by low background seismicity rates, detecting induced events in California hydrocarbon basins received less attention, despite extensive injection operations and seismically active faults. Up to now, few injection-induced earthquakes outside of geothermal reservoirs have been observed in California [*Kanamori and Hauksson*, 1992; *Goebel et al.*, 2015]. Consequently, the most acute anthropogenically controlled seismic hazard stems from fluid-injection activity close to active faults. Such injection activity can lead to earthquakes up to M_w5.7 or larger as observed in OK [*Keranen et al.*, 2013].

In California, annual fluid-injection volumes exceed those in OK where induced seismicity is suggested to be widespread. The average number of active injection wells between 2010 and 2013 of ~9900 exceeds the ~8600 wells in OK [*CA Department of Conservation*, 2012]. The wells in California inject on average at depth of ~1.5 km which is about 0.5 km deeper than in OK [*Goebel*, 2015]. More recently and coincident with continuously increasing oil prices between 2001 and 2014 (except 2009 and 2010), California experienced a systematic increase in injection volumes in connection with more extensive well-stimulation operations. This increase

in injection activity together with the lack of available injection sites away from active faults requires a more detailed assessment of possible seismogenic consequences of fluid injection in California.

This study is structured as follows: we first provide an overview of the geologic setting, as well as injection and seismic activity at the southern end of the Central Valley. This is followed by a detailed assessment of the seismically active faults within the study region. We then investigate a possible correlation between fluid injection and seismicity, including variations in frequency-magnitude distribution with the onset of injection rate increase. Lastly, we create a detailed hydrogeological model that incorporates local geology such as active fault structures and examine injection-induced pressure changes.

2. Swarm Activity, Wastewater Disposal Operations, and Geological Setting

This study concentrates on a potentially injection-induced earthquake swarm in 2005, which is associated with the White Wolf fault (WWF) and occurred at the southern end of the Central Valley, CA. The swarm, which is referred to as White Wolf swarm in the following, deviates from standard main shock-aftershock patterns. It is comprised of a M_L4.5 event on 22 September, followed by two M_L4.7 (M_w4.6) and M_L4.3 events the same day as well as some smaller magnitude "fore shocks." The White Wolf swarm is suspected to be connected to fluid-injection activity based on a statistical assessment of injection and seismicity rate changes [*Goebel et al.*, 2015]. The statistical assessment showed that an abrupt increase in injection rates in 2005 was followed by a large increase in seismicity rates, which exceeded the 95% confidence interval of previous rate variations since 1980. In other words, the area did not experience a comparable rate increase within a 10 km radius of the well prior to the start of injection in 2005. Moreover, the strong correlation between rapid injection rate changes and the subsequent seismicity sequence had a ≈3% probability of coinciding by chance based on tests with randomly determined onsets of injection rate changes [*Goebel et al.*, 2015].

The White Wolf swarm occurred at the southern end of Kern County, the largest oil-producing (>75% of the state's oil production) and fluid-injecting (>80% of all injection wells) county in California [*CA Department of Conservation*, 2012]. The region experienced one major earthquake since 1950, i.e., the 1952, M_w7.3 Kern county event, and hosts many seismically active faults including the White Wolf, Wheeler Ridge, and Pleito faults (Figure 1a).

Fluid injection rates at the southern end of the Central Valley increased rapidly from ~20,000 to more than 100,000 m^3/mo between 2001 and 2010 (Figure 1b). The majority of wastewater, i.e., 80 to 95%, was injected within the Tejon Oil Field involving only three closely spaced wells. These wells started injecting in 2001 (WD01), 2004 (WD04), and 2005 (WD05), and injection fluids were generally contained below 950 m. Effective well depths are reported between ~1200 and ~1500 m [*CA Department of Conservation*, 2012]. The injection wells targeted a 25–30 m thin, highly permeable ($0.2–1.0 \cdot 10^{-12}$ m^2) stratigraphic zone within the Monterey formation [*CA Department of Conservation*, 2012]. This injection zone is composed of turbiditic sand lenses with maximum lateral extents of 1 to 2 km (Figure S2 in the supporting information). Moreover, the wellbores include a significant, horizontally drilled portion with 520 to 580 m long perforation zones that maximized injection rates.

Injection into well WD05 occurred at consistently high rates of ~57,000 m^3/mo, starting 5 months before the White Wolf swarm in September 2005. During these five months, the wellbore accommodated more than 75% of the total injection activity of the entire study area. WD05 is located in an area of closely spaced, northwest striking, Early Miocene, buried, normal faults that show evidence of local Holocene reactivation. Based on geological mapping, seismicity, and well-log data, we identified a seismically active normal fault located between the WWF and injection site WD05 (Figure 1a, see supporting information Text S1 and Figures S1–S3 for details of fault identification). This fault is referred to as "Tejon fault" in the following text. Both seismicity and well-log data suggest that the Tejon fault is shallow close to the injection site and deepens toward the northwest below the Wheeler Ridge fault before intersecting with the WWF (Figure 1c). The horizontally elongated perforation zone of well WD05, which extends directly east from the well head, increased the probability of intersecting the Tejon fault with the borehole.

3. Seismicity Analysis and Hydrogeological Modeling

The White Wolf swarm shows evidence of systematic event migration between injection sites and the M_w4.6 hypocenter (Figures 1c and 2). This systematic migration is best seen in relocated catalogs that include newly

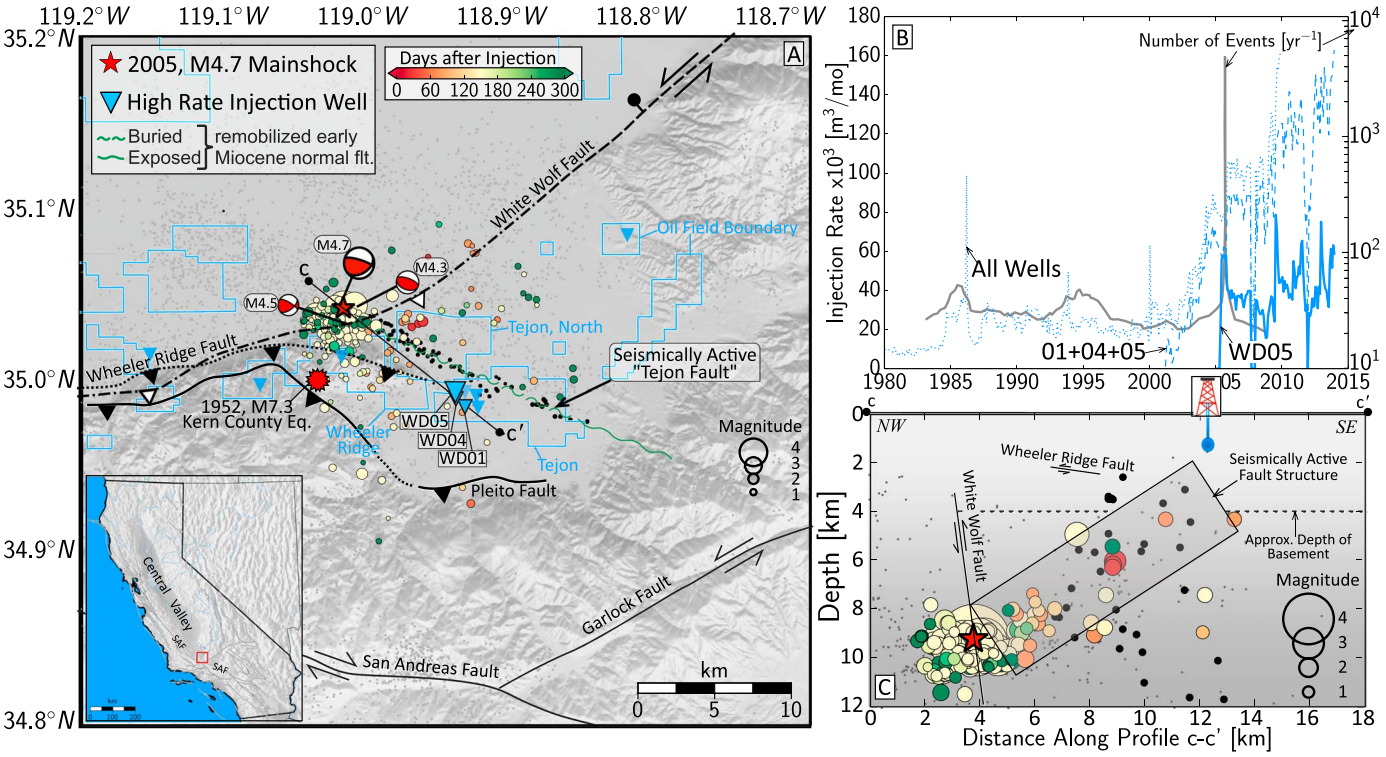

Figure 1. Seismicity and injection activity within the study area centered at the Tejon Oil Field. (a) Fault traces (black and green lines), epicenters (dots), injection wells (blue triangles), and oilfield locations (blue lines). Seismicity is colored according to days after injection into WD05, gray dots show background seismicity. Earthquake locations are from the standard Southern California Seismic Network (SCSN) catalog. (b) Injection (blue) and seismicity rates (gray) between 1980 and 2014. (c) Seismicity cross section within a 5 km zone between c and c′ in Figure 1a. Seismicity up to 300 days after the start of injection is shown in colored dots (see colorbar in Figure 1a), background events by gray dots, and Tejon fault seismicity prior to injection by black dots. The gray rectangle qualitatively highlights a zone of high seismic activity that coincides with the Tejon fault. Earthquake locations are based on a high-quality waveform relocated catalog [*Shearer et al.*, 2005].

detected events using a template-matching method and may easily remain undetected in standard seismicity catalogs (Figure 2). Within the first 2 months of wastewater disposal in WD05, we observed some shallow seismicity at 4 km depth beneath the injection site and on the Tejon fault to the northwest, while little to no seismic activity occurred to the south and southeast. Within the following months, the area northwest of well WD05 in direction of the WWF became progressively active. Much of this seismicity was concentrated just updip of the intersection point between the Tejon and White Wolf fault between ~70 and 150 days after injection (see animations in the supporting information).

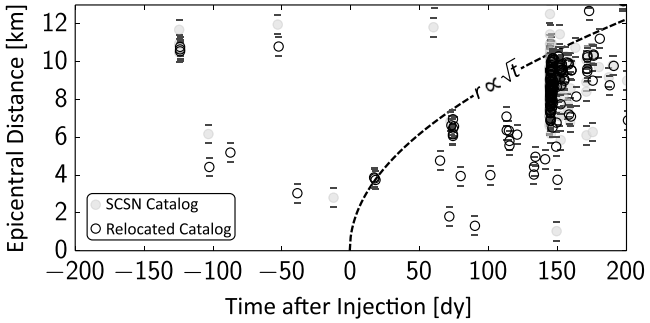

Figure 2. Seismicity migration along the Tejon fault relative to the start of injection in WD05. We show both the SCSN (gray dots) and relocated earthquake catalogs (black circles). The latter includes new event detections using a template-matching approach. Epicentral distances are reported relative to well-head location, error bars show average, absolute location uncertainties. The dashed curve highlights the expected trend for a square-root dependence of distance on time characteristic for a diffusive process.

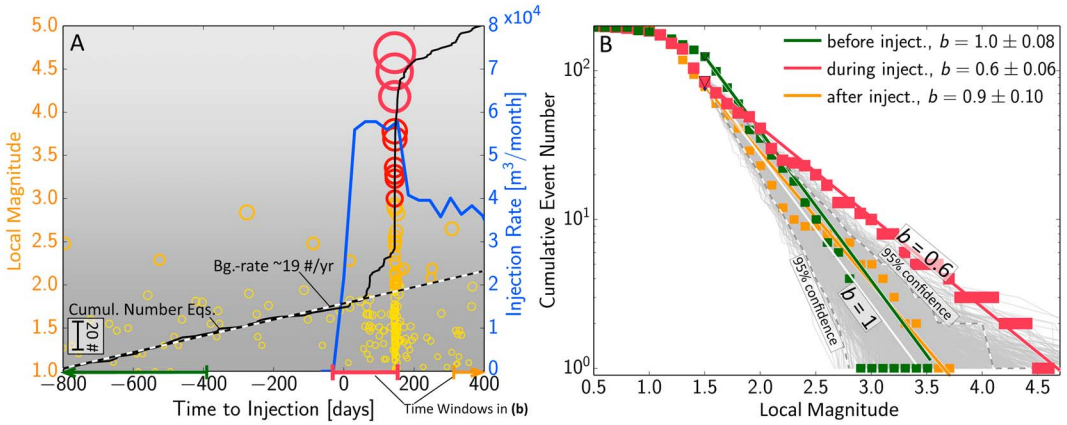

Figure 3. Fluid injection rates in well WD05, seismic activity, and frequency-magnitude distributions (FMDs) of the likely induced White Wolf swarm. (a) Injection rates (blue), cumulative number of earthquakes (black), and event magnitudes (circles) within a 10 km radius of injection in well WD05. (b) FMD before (green), during (red), and after (orange) peak injection rates as well as 95% confidence interval for a FMD with $b = 1$.

In the two years prior to injection into WD05, seismicity rates within a 10 km radius of the well were largely constant (Figure 3a). The start of injection also marked the onset of seismicity rate increase which peaked about 150 days later. The occurrence of the three M_L >4 events was closely followed by a ~30% decrease in injection rates in well WD05 and injection rates kept decreasing over the ensuing 4 years.

In addition to seismicity rate changes, the frequency-magnitude distribution (FMD) strongly deviated from expected behavior of Gutenberg-Richter-type FMDs with *b* values close to unity (Figure 3b). During the period of peak injection in WD05 the *b* value within a 10 km radius was 0.6. This value was significantly lower than before (b=1) and after (b=0.9) peak injection activity. Moreover, we observed a long-term decrease in *b* value coincident with a rate increase in cumulative injection rates in WD01, WD04, and WD05 (Figure S4). Using Monte Carlo simulations of earthquake magnitudes based on the observed *a* value, magnitude of completeness of 1.5, we compute the 95% confidence interval of FMDs with b=1. The observed FMD exceeds the upper confidence bound, indicating a significantly larger proportion of large-magnitude events during the White Wolf swarm which is also confirmed by the corresponding moment magnitudes for events above *M*4 (see supporting information Text S1 for details on moment magnitude computations). Decreasing and low *b* values may be characteristic for gradual fault activation processes, observed in laboratory experiments [*Goebel et al.*, 2013] and during fluid injection [e.g., *Maxwell et al.*, 2009; *Skoumal et al.*, 2014; *Huang and Beroza*, 2015].

To further test if the 2005 White Wolf swarm was connected to wastewater disposal, we model permeability structure and pressure diffusion close to the injection site. Pressure diffusion was likely influenced by high permeability along the seismically active part of the Tejon fault located N-W of well WD05. Slip along this fault may have been pivotal in maintaining elevated permeability down to the depth of the White Wolf swarm. The existence of a zone with higher permeability than the surrounding lithology is supported by several observations such as follows:

1. The asymmetric seismicity distribution concentrated N-W of well WD05 with little to no seismicity to the south and east of the injection sites. Most of these events occurred at depths between the M_w4.6 hypocenter and the injection depth (Figure S5).
2. The presence of background seismic activity on the upper portion of the Tejon fault revealing that part of the fault was seismically active prior to injection.
3. The presence of several mapped faults and fracture zones located N-W of the injection site between WD05 and WWF (Figure S3).

Our 3-D numerical diffusion model includes three principal stratigraphic zones, in addition to the Tejon fault which is implemented as a vertical zone of elevated permeability (Figure 4a). These three zones are (1) the injection zone, i.e., a 20–30 m thin turbiditic sand lens in the Monterey formation with a lateral extent of up to ~1.5 km, labeled as "Transition zone" in the industry data [*CA Department of Conservation*, 2012]; (2) the crystalline (gneissic) basement complex, and (3) the Monterey formation. Permeability is high within the sand

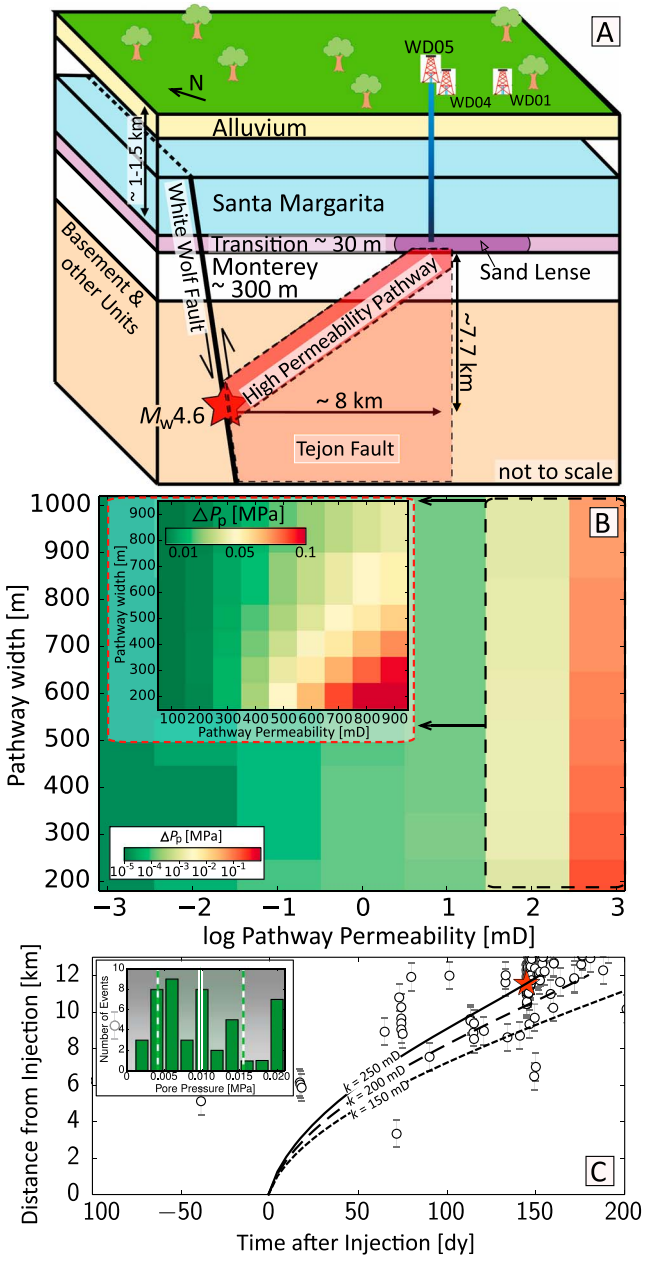

Figure 4. Hydrogeological modeling and predicted pore pressure increase caused by injection in well WD05. (a) Schematic representation of model setup including the high-permeability zone between injection site and M_w4.6 event. The hydrogeological model is based on geologic mapping and industry data described in Text S1 in the supporting information. (b) Model-dependent pore pressure change (ΔP_p) at distance of the M_w4.6 event (~11 km) for different values of fault zone width and permeability. (c) Observed hypocenter migration along the Tejon fault zone (black circles). The theoretical position of a 0.01 MPa pressure front is shown for a 500 m wide fault zone and three different permeability values (150, 200, and 250 mD). The M_w4.6 event is shown by a red star. The inset shows distribution of pore pressures at each hypocenter for $k = 200$ mD and $w = 500$ m, vertical lines are mean and standard deviation.

lenses (i.e. ~1 D) and very low (~10^{-4} mD) above injection depth which is one of the requirements for the selection of an injection site. Similarly, permeability is low (~10^{-4} mD) within the basement and Monterey formations outside of the injection zone (permeabilities are reported in millidarcy, 1 mD ≈10^{-15} m^2).

Our hydrogeological model is based on the most complete available data sets within the upper ~2–3 km of sedimentary basins and includes seismicity records, geologic mapping results, and industry data (i.e., well logs, stratigraphic columns, and interpreted reservoir structure, see supporting information Text S1).

Below these depths, few geophysical data are available except for the seismicity record. To account for larger uncertainty at these depths, we chose a coarse modeling scale which primarily resolves the influence of large-scale structural heterogeneity such as large fault zones. More detailed information about the model setup can be found in the supporting information Text S1.

Our modeling results show that thin fault zones with higher permeability lead to fluid-pressure increase sufficient to trigger earthquakes at distances similar to the M_w4.6 hypocenter. We performed a detailed sensitivity analysis of pressure changes resulting from varying fault zone width and permeability. Permeability was varied over 7 orders of magnitude between 10^{-3} to 10^3 mD to account for generally large uncertainties in permeability measurements [*Manga et al.*, 2012], and fault width was varied between 100 and 1000 m (Figure 4b and supporting information Table S1). The modeled pressure changes experienced by a fault at ~11 km distance span 4 orders of magnitude depending on the initial conditions, with significantly stronger effects of permeability changes compared to variations in fault zone width (Figure 4b). For fault zone permeability above ~300 mD and fault width below ~800 m, we observe a pressure increase at the M_w4.6 hypocenter of at least 0.01 MPa (Figure 4b), which is sufficient to induce seismicity on faults favorably oriented to slip [*Keranen et al.*, 2014; *Hornbach et al.*, 2015]. Fault zones with lower permeability may result in similar magnitude pressure changes if they are sufficiently narrow. The here described seismogenic consequences of thin, high-permeability pressure channels are in agreement with previous studies of induced seismicity in Colorado and Arkansas [*Hsieh and Bredehoeft*, 1981; *Zhang et al.*, 2013].

The migration pattern of seismic events relative to injection into WD05 can be used to constrain a plausible range of permeability values by correlating seismicity and modeled pressure front location along the Tejon fault (Figure 4c). The shape of the pore pressure front in a distance-time plot depends on the particular reservoir geometry and permeability values with a commonly observed square-root dependence of distance on time for simple radial symmetric models (Figure 2) [*Talwani and Acree*, 1984; *Shapiro et al.*, 1997]. Using the more complex 3-D reservoir and fault geometries in our model, we find that fault zone permeability between 150 and 250 mD and a width smaller than 500 m best agrees with the observed seismicity for a change in fluid pressure of 0.01 MPa. This is within the general range of fault zone permeability values inferred from seismicity migration [e.g., *Ingebritsen and Manning*, 2010; *Manga et al.*, 2012]. Much of the seismicity occurred close to the arrival of the initial pressure pulse of ~0.01 MPa, indicating that faults within the area may have been critically stressed, i.e., stress levels were within a narrow range below the shear strength (Figure 4c inset).

4. Discussion

The identification of human-induced earthquakes in tectonically active regions such as California is generally complicated by the many naturally occurring seismicity sequences. To address these challenges, we used detailed statistical analysis methods [*Goebel et al.*, 2015] as well as geological and diffusion models to evaluate a potentially induced origin of an earthquake sequence close to the WWF in 2005. This sequence deviates from commonly observed tectonic sequences in the area by showing significantly elevated seismicity rates above the background associated with a rapid increase in injection rates. Moreover, the seismicity sequence showed evidence for deep migration within the crystalline basement between injection wells and the nearby White Wolf fault suggesting that wastewater disposal likely contributed to triggering the earthquake swarm. The recorded largest magnitude event (M_{max}=4.6) of the sequence and the cumulative injection volume (V_{tot} ~$1.8 \cdot 10^6$ m^3) fall well within the trend of V_{tot} and M_{max} reported by *McGarr* [2014] and are similar to observations of V_{tot} and M_{max} in Timpson, Texas, and Painesville, Ohio [*McGarr*, 2014]. This analysis assumes that injection in all three wells (WD01, WD04, and WD05) contributed to the induced seismicity sequence.

Our results highlight that injection related earthquake triggering processes may involve multiple mechanisms. A plausible mechanism for the triggering of the White Wolf swarm is the diffusion of pressures from the ~1.5 km deep injection site along the northwest striking Tejon fault into the intersection zone with the WWF. This pressure channeling effect may have been further intensified if the WWF acted as flow barrier, thereby trapping the pressure front within the damage zone of the Tejon fault resulting in more rapid pressure increase at the intersection between the two faults. Other triggering mechanisms may have included stress transfer at the front of the pressurized zone as well as injection-induced aseismic slip, which progressively became more seismogenic at larger depth within the basement complex. Shallow aseismic slip is well documented in high-resolution, controlled injection experiments and may hide early fault activation processes [*Cornet et al.*, 1997; *Guglielmi et al.*, 2015]. A potentially injection-induced origin of the White Wolf swarm is intrinsically

connected to the specific geologic setting that accommodated pressure diffusion to seismogenic depth at the southern end of the Central Valley. More detailed assessments of the geologic setting close to injection wells are required to explain the lack of large-scale injection-induced earthquake activity in California hydrocarbon basins [*Goebel*, 2015].

Cases of relatively deep induced seismicity far from injection sites have been reported in several other regions such as Oklahoma, Colorado, and Arkansas, where induced earthquakes occurred at 8 km depth and 7 to 35 km distance from the injection well [*Hsieh and Bredehoeft*, 1981; *Horton*, 2012; *Keranen et al.*, 2014]. In addition to these large distances, there are several other factors that can complicate induced seismicity detection in California hydrocarbon basins: (1) Faults may channel induced pressure changes and lead to localized pore pressure increase; (2) background seismicity rates are generally high so that small-rate variations cannot be detected; (3) small-magnitude earthquakes close to injection sites can easily be missed because of sparse station coverage within hydrocarbon basins; and (4) transient aseismic and seismic slip processes lead to a dynamic increase in permeability and progressive fault activation [*Cornet et al.*, 1997; *Bourouis and Bernard*, 2007; *Guglielmi et al.*, 2015; *Wei et al.*, 2015]. All of these factors can potentially complicate mitigation strategies such as traffic light systems which rely on a systematic seismicity rate increase and event migration from the well.

Based on our empirical results, injection-induced earthquakes are expected to contribute marginally to the overall seismicity in California [see also *Goebel*, 2015; *Goebel et al.*, 2015]. This is in line with physical models of crustal strength distributions which suggest a limit to the amount of strain energy that is available for shallow earthquake ruptures [e.g., *Sibson*, 1974]. Moreover, the frictional properties of shallow, sedimentary faults inhibit rupture growth and diminish the seismogenic impact of surficial pressure perturbation [e.g., *Das and Scholz*, 1983]. However, considering the numerous active faults in California, the seismogenic consequences of even a few induced cases can be devastating.

5. Conclusion

Wastewater injection-induced earthquakes are rare in California compared to widespread tectonic seismicity. Nevertheless, the proximity of high-rate injectors and large active faults can cause noticeable earthquakes under certain geologic conditions. Our results suggest a connection between wastewater disposal and seismicity with events up to M_w4.6 at the southern end of the Central Valley. Wastewater injection within this region should be monitored carefully because of the presence of high-permeability fault structures that connect the injection site with the nearby WWF. The relatively shallow crystalline basement south of the WWF may increase the probability of inducing earthquakes, if fluids migrate beyond the intended geologic formations.

The present example shows that injection-induced earthquakes may remain unidentified in tectonically active regions if only standard seismicity catalogs with comparably high magnitudes of completeness are analyzed. We present a pathway to more reliable identification of possibly induced earthquakes by extending the seismicity records to lower magnitudes and by analyzing waveform relocated catalogs as well as hydrogeological models. Such a detailed analysis of the available data may help recognize regions with increased induced seismicity potential and prevent injection-induced seismicity in California in the future.

Acknowledgments
The authors thank Semechah Lui, Preston Jordan, Bill Foxall, Emily Brodsky, and members of the Induced Seismicity Consortium at USC for helpful comments and discussions. The manuscript benefitted from comments by Art McGarr and Michael Wysession. The well and operational data were supplied by the California Department of Conservation (www.doggr.com), and the seismicity data by the Southern California Earthquake Center (doi: 10.7909/C3WD3xH1) and Advanced National Seismic Systems. This study was funded by NEHRP/USGS grants G14AP00075 and G15AP00095 to Caltech, by the Southern California Earthquake Center (SCEC) under contribution numbers 12017 and 15168 and the Induced Seismicity Consortium (ISC) at USC.

References

Bourouis, S., and P. Bernard (2007), Evidence for coupled seismic and aseismic fault slip during water injection in the geothermal site of Soultz (France), and implications for seismogenic transients, *Geophys. J. Int.*, *169*(2), 723–732.

CA Department of Conservation (2012), Division of oil, gas and geothermal resources: Production history in California. [Available at ftp://ftp.consrv.ca.gov/pub/oil/annual_reports, accessed Sept. 26, 2014.]

Cornet, F., J. Helm, H. Poitrenaud, and A. Etchecopar (1997), Seismic and aseismic slips induced by large-scale fluid injections, *Pure Appl. Geophys.*, *150*, 563–583.

Das, S., and C. Scholz (1983), Why large earthquakes do not nucleate at shallow depths, *Nature*, *305*, 621–623.

Ellsworth, W. L. (2013), Injection-induced earthquakes, *Science*, *341*(6142), 1225942.

Frohlich, C., and M. Brunt (2013), Two-year survey of earthquakes and injection/production wells in the Eagle Ford Shale, Texas, prior to the M_W 4.8 20 October 2011 earthquake, *Earth Planet. Sci. Lett.*, *379*, 56–63.

Goebel, T. H. W. (2015), A comparison of seismicity rates and fluid injection operations in Oklahoma and California: Implications for crustal stresses, *Leading Edge*, *34*(6), 640–648, doi:10.1190/tle34060640.1.

Goebel, T. H. W., D. Schorlemmer, T. W. Becker, G. Dresen, and C. G. Sammis (2013), Acoustic emissions document stress changes over many seismic cycles in stick-slip experiments, *Geophys. Res. Lett.*, *40*, 2049–2054, doi:10.1002/grl.50507.

Goebel, T. H. W., E. Hauksson, F. Aminzadeh, and J.-P. Ampuero (2015), An objective method for the assessment of possibly fluid-injection induced seismicity in tectonically active regions in central California, *J. Geophys. Res. Solid Earth*, *120*, 7013–7032, doi:10.1002/2015JB011895.

Guglielmi, Y., F. Cappa, J.-P. Avouac, P. Henry, and D. Elsworth (2015), Seismicity triggered by fluid injection-induced aseismic slip, *Science*, *348*(6240), 1224–1226.
Healy, J., W. Rubey, D. Griggs, and C. Raleigh (1968), The Denver earthquakes, *Science*, *161*(3848), 1301–1310.
Hornbach, M. J., et al. (2015), Causal factors for seismicity near Azle, Texas, *Nat. Commun.*, *6*, 6728.
Horton, S. (2012), Disposal of hydrofracking waste fluid by injection into subsurface aquifers triggers earthquake swarm in central Arkansas with potential for damaging earthquake, *Seismol. Res. Lett.*, *83*(2), 250–260.
Hsieh, P. A., and J. D. Bredehoeft (1981), A reservoir analysis of the Denver earthquakes: A case of induced seismicity, *J. Geophys. Res.*, *86*(B2), 903–920.
Huang, Y., and G. C. Beroza (2015), Temporal variation in the magnitude-frequency distribution during the Guy-Greenbrier earthquake sequence, *Geophys Res. Lett.*, *42*, 6639–6646, doi:10.1002/2015GL065170.
Ingebritsen, S., and C. Manning (2010), Permeability of the continental crust: Dynamic variations inferred from seismicity and metamorphism, *Geofluids*, *10*(1–2), 193–205.
Kanamori, H., and E. Hauksson (1992), A slow earthquake in the Santa Maria Basin, California, *Bull. Seismol. Soc. Am.*, *82*(5), 2087–2096.
Keranen, K., M. Weingarten, G. Abers, B. Bekins, and S. Ge (2014), Sharp increase in central Oklahoma seismicity since 2008 induced by massive wastewater injection, *Science*, *345*(6195), 448–451.
Keranen, K. M., H. M. Savage, G. A. Abers, and E. S. Cochran (2013), Potentially induced earthquakes in Oklahoma, USA: Links between wastewater injection and the 2011 M_w 5.7 earthquake sequence, *Geology*, *41*(6), 699–702.
Kim, W.-Y. (2013), Induced seismicity associated with fluid injection into a deep well in Youngstown, Ohio, *J. Geophys. Res. Solid Earth*, *118*, 3506–3518, doi:10.1002/jgrb.50247.
Manga, M., I. Beresnev, E. E. Brodsky, J. E. Elkhoury, D. Elsworth, S. Ingebritsen, D. C. Mays, and C.-Y. Wang (2012), Changes in permeability caused by transient stresses: Field observations, experiments, and mechanisms, *Rev. Geophys.*, *50*, RG2004, doi:10.1029/2011RG000382.
Martínez-Garzón, P., G. Kwiatek, H. Sone, M. Bohnhoff, G. Dresen, and C. Hartline (2014), Spatiotemporal changes, faulting regimes, and source parameters of induced seismicity: A case study from the Geysers Geothermal Field, *J. Geophys. Res. Solid Earth*, *119*, 8378–8396, doi:10.1002/2014JB011385.
Maxwell, S. C., et al. (2009), Fault activation during hydraulic fracturing, paper presented at 2009 SEG International Exposition and Annual Meeting, Houston, Tex., 25–30 Oct.
McGarr, A. (2014), Maximum magnitude earthquakes induced by fluid injection, *J. Geophys. Res. Solid Earth*, *119*, 1008–1019, doi:10.1002/2013JB010597.
Rubinstein, J. L., W. L. Ellsworth, A. McGarr, and H. M. Benz (2014), The 2001-present induced earthquake sequence in the Raton Basin of northern New Mexico and southern Colorado, *Bull. Seismol. Soc. Am.*, *104*, 2162–2181.
Schoenball, M., L. Dorbath, E. Gaucher, J. F. Wellmann, and T. Kohl (2014), Change of stress regime during geothermal reservoir stimulation, *Geophys. Res. Lett.*, *41*, 1163–1170, doi:10.1002/2013GL058514.
Shapiro, S. A., E. Huenges, and G. Borm (1997), Estimating the crust permeability from fluid-injection-induced seismic emission at the KTB site, *Geophys. J. Int.*, *131*, F15–F18.
Shearer, P., E. Hauksson, and G. Lin (2005), Southern California hypocenter relocation with waveform cross-correlation, Part 2: Results using source-specific station terms and cluster analysis, *Bull. Seismol. Soc. Am.*, *95*(3), 904–915.
Sibson, R. H. (1974), Frictional constraints on thrust, wrench and normal faults, *Nature*, *249*, 542–544.
Skoumal, R. J., M. R. Brudzinski, B. S. Currie, and J. Levy (2014), Optimizing multi-station earthquake template matching through re-examination of the Youngstown, Ohio, sequence, *Earth Plant. Sci. Lett.*, *405*, 274–280, doi:10.1016/j.epsl.2014.08.033.
Talwani, P., and S. Acree (1984), Pore pressure diffusion and the mechanism of reservoir-induced seismicity, *Pure Appl. Geophys.*, *122*(6), 947–965.
Wei, S., et al. (2015), The 2012 Brawley swarm triggered by injection-induced aseismic slip, *Earth Planet. Sci. Lett.*, *422*, 115–125.
Zhang, Y., et al. (2013), Hydrogeologic controls on induced seismicity in crystalline basement rocks due to fluid injection into basal reservoirs, *Groundwater*, *51*(4), 525–538.